Assessment of Energy Storage Potential for System Inertia and Primary Frequency Response

Priyanka Kushwaha[1], Vivek Prakash[2], Rohit Bhakar[1], Udaykumar R Yaragatti[1], Anjali Jain[3] and Yamujala Sumanth[3]

Department of Electrical Engineering[1], Centre for Energy & Environment[3]
Malaviya National Institute of Technology Jaipur, India
School of Automation[2], Banasthali Vidyapith, India
Email: rbhakar.ee@mnit.ac.in

***Abstract*—Intermittency and uncertainty associated with renewable energy sources (RES) such as solar and wind would have an adverse impact on system frequency. These impacts could be recurring events of frequency deviation followed by inevitable contingencies that may endanger system security. Hence, post-fault frequency stability is essential for secure system operations. The initial frequency deviation can be arrested by adequate system inertia (SI) and primary frequency response (PFR). In this context, this paper investigates the potential of pumped hydro energy storage (PHES) for SI and PFR under large RES integration. Generation scheduling is performed for the day-ahead, to estimate the PFR requirement. The study would envisage the role of PHES for inertia response and PFR, to mitigate generation-demand balance followed by sudden loss of the largest generation unit. Frequency security parameters like the rate of change of frequency (RoCoF), nadir frequency and quasi-steady-state frequency value are examined for PFR adequacy assessment. Case studies are carried out on New-England 10 machine test system, to demonstrate the efficacy of the proposed model.**

Keywords— Frequency dynamics Primary Frequency response, renewable energy sources, system inertia.

I. INTRODUCTION

System inertia (SI) and governor response was inherently available in abundance, hence given little attention in system operation [1]. However, the increasing generation share from renewable energy sources (RES), synchronous generators (SG) are being displaced. Moreover, the integrated solar and wind plants provide zero or weak SI and primary frequency response (PFR), due to their power electronic converter-based grid interface. This necessitates increased requirement of inertial response and PFR under large RES integration, to control post fault frequency dynamics.

The increased SI and PFR requirement necessitate incorporation of frequency constraints in generation scheduling [2]. This constraints under large RES generation could be performed to accurately estimate the required response under inevitable events like largest generator outage. However, large integration of RES generation may violate prescribed frequency security limit due to associated intermittency and variability. This violation may lead to emergency control like under frequency load shedding (UFLS). In order to maintain the system security, additional SG need to be scheduled to meet the increased system frequency response. This additional committed units, results in increase of system operating cost and RES curtailment to control generation-demand balance. Therefore, to ensure inertial and PFR adequacy under large RES integration, assimilation of quick responding energy storage systems (ESS) is essential.

The ESS with adequate energy density and fast response charactertics like PHES and battery energy storage system (BESS) can counteract generation-demand imbalances [3-6] and improve system frequency response [7-8]. This paper focused on established energy storage technology PHES. The 99% of the available bulk EES capacity globally is PHES, with around 125GW capacity [9]. The PHES is a flexible resource can counteract generation-demand imbalance during contingency event [10]. The integration of adjustable speed (AS) and ternary in PHES improves its efficiency as well provides operational flexibility. These development results in power adjustments during pumping and turbine mode and facilitate PHES to provide PFR [11]. The fixed speed and ternary units in PHES are inherent sources of inertia due to their rotating generator. Thus, PHES in the system can be beneficial for system frequency security under variable RES generation. The application of PHES may be constrained by its available capacity during dispatch. Thus to assure the inertia and PFR adequacy, requires incorporation of PHES in generation scheduling. The scheduling of PHES in a day-ahead and secondary reserve market is formulated [12]. However, post fault frequency constraints are not considered. These, constraints are modelled and impact of wind uncertainty on system inertia is assed at fixed penetration level [13]. However, there is need to investigate the potential of PHES at different integration of RES (wind and PV) generation to analyze the SI and PFR requirement.

In this context, paper proposes a PFR constrained generation scheduling in day-ahead to assess the potential of PHES for inertia and PFR support under large RES integration. The study is analyzed the system frequency behavior under largest generator outage. The post fault frequency constraints like rate of change of frequency (RoCoF), frequency nadir and steady-state frequency are examined. Further the study inspects the impact of frequency constraints on RES power and operating cost. Proposed methodology provides an understanding of system behavior with large RES generation, with the overall response requirement. The participation of PHES for SI and PFR under different integration of RES is examined. The present study will help the system operator to handle system under contingency and during imbalances.

This work is supported by the DST grant for UKICERI project, DST/RCUK/JVCCE/2015/02.

The organization of paper is as follows: section-II introduces the frequency response constrained in generation scheduling incorporating PHES, section-III covers the case study and simulation results followed by conclusion in section-IV.

II. PROBLEM FORMULATION

The generations scheduling is modified in a way to incorporate PHES, SI and PFR constraints under large RES integration. The objective is to minimize overall cost of the system as given in (1). The objective function constitutes the conventional units operating cost along with start-up and shut-down cost. Along with curtailment cost of load and renewables generation. In first part of (1), a,b,c denotes the cost coefficients of thermal units, C^u & C^d denotes start-up and shut-down cost, $P_{g,t}$ is generating power of unit g at time t .Second term has *VOLL* as value for load-shed LS_t at time t . Whereas in third and fourth term, $P^{cur}_{pv,t}$ & $P^{cur}_{wind,t}$ denotes curtailed PV and wind power at time t with curtailment cost of $C^{cur}_{pv,t}$ & $C^{cur}_{wind,t}$ respectively.

$$\min TC = \sum_{i}^{I}\sum_{t}^{T} a.P_{g,t}^2 + b.P_{g,t} + c + C^u + C^d + \sum_{t}^{T} VOLL.LS_t + \sum_{pv}^{PV}\sum_{t}^{T} P^{cur}_{pv,t}.C^{cur}_{pv,t} + \sum_{w}^{W}\sum_{t}^{T} P^{cur}_{w,t}.C^{cur}_{w,t} \quad \forall g,t \tag{1}$$

A. Generation scheduling

The basic constraints for scheduling conventional units in day-ahead is formulated from (2)-(8). Depending upon the units status at t and $t-1$, unit's start-up and shut-down status is decided by (2) where $\alpha_{g,t}, \beta_{g,t}$ & $\chi_{g,t}$ are unit's on, start-up and shut-down status. Constraint (3) restricts individual unit to go in start-up and shut-down simultaneously.

$$\beta_{g,t} - \chi_{i,t} = \alpha_{g,t} - \alpha_{g,t-1} \quad \forall g,t \tag{2}$$

$$\beta_{g,t} + \chi_{g,t} \le 1 \quad \forall g,t \tag{3}$$

The minimum up $UT_{g,t}$ and down time $DT_{g,t}$ of the conventional units is constrained by (4), (5) & (6), (7) respectively.

$$\beta_{g,t} \le \alpha_{g,t} + UT_{g,t_1} \quad \forall i,t \tag{4}$$

$$UT_{g,t} = \begin{cases} t_1 & t_1 \le t_g^{off} \\ 0 & t_1 > 0 \end{cases} \quad \forall g \tag{5}$$

$$\chi_{g,t} + U_{g,t} + DT_{g,t_1} \le 1 \quad \forall g,t \tag{6}$$

$$DT_{g,t_1} = \begin{cases} t_1 & t_1 \le t_g^{off} \\ 0 & t_1 > t_g^{off} \end{cases} \quad \forall g \tag{7}$$

The unit's generation at time t is bounded by its maximum ramp-up $\bar{R}_g^{up}$ and ramp-down $\bar{R}_g^{dw}$ limit as in (8) & (9) respectively.

$$P_{g,t} - P_{g,t-1} \le \bar{R}_g^{up} \quad \forall g,t \tag{8}$$

$$P_{g,t-1} - P_{g,t} \le \bar{R}_g^{dw} \quad \forall g,t \tag{9}$$

The power flow from line i to line j is controlled by its angle δ_i, δ_j and reactance x_{ij} at time t as mention in (10). The branch power flow limit is mention in (11), limited by power transmission capability. Constraint (12) limit the maximum power generation from unit g at time t .

$$P_{ij,t} = \frac{\delta_{i,t} - \delta_{j,t}}{x_{ij,t}} \quad \forall ij \in \Omega_l \tag{10}$$

$$-P_{ij}^{max} \le P_{i,t} \le P_{ij}^{max} \tag{11}$$

$$\underline{P}_g \le P_{g,t} \le \bar{P}_g \tag{12}$$

B. Primary Frequency Response

The formulation for system inertia SI and PFR is given from (13)-(21). The system's obligation on PFR requirement pfr_t^{tot} should be greater than 50% of generation loss ΔP^l at time t mention in (13). The PFR from conventional units $pfr_{g,t}$ is constrained by generator maximum limit (14).

$$pfr_t^{tot} \ge 50\% \left(\Delta P^l\right) \quad \forall t \tag{13}$$

$$pfr_{g,t} + P_{g,t} \le \bar{P}_g \alpha_{g,t} \quad \forall i,t \tag{14}$$

The inertia from conventional unit $Sys_{g,t}^{iner}$ in (15) depend upon generation maximum capacity $\bar{P}_g$, inertia constant H_g and nominal frequency f_0 . The rate of change of frequency $RoCoF_t$ is dependent on system inertia Sys_t^{tot} and it is bounded based on permissible limit as in (16).

$$Sys_{g,t}^{iner} = \frac{\sum_g^G \bar{P}_g H_g \ \alpha_{g,t}}{f_0} \quad \forall t \tag{15}$$

$$RoCoF_t = \frac{-\Delta P^l}{2\, Sys_t^{tot}} \le \overline{RoCoF} \quad \forall t \tag{16}$$

Constraints (17)-(19), calculates frequency nadir f_t^n , nadir time t^n and assess the PFR contribution based on unit's governor ramping capability mention in (19). Here, Δf^{db} and f^{ufls} is governor dead band and UFLS frequency limit respectively.

$$f_t^n = f_0 - \Delta f^{db} - \frac{f_0 \left(\Delta P^l\right)^2}{4 \sum_g^G \bar{P}_g \ H_g \ \alpha_{g,t} \ R_g^{up}} \tag{17}$$

$$t^n \le \frac{4\sum_{g}^{G} Sys_{g,t}^{iner}\left(f_0 - \Delta f^{db} - f^{ufls}\right)}{f_0\ \Delta P^l} + \frac{2\sum_{g}^{G} Sys_{g,t}^{iner}\Delta f^{db}}{f_0\ \Delta P^l} \quad (18)$$

$$\sum_{g}^{G} pfr_{g,t} \le R_g^{up,gov}\left[\frac{4\sum_{g}^{G} Sys_{g,t}^{iner}\left(f_0 - \Delta f^{db} - f^{ufls}\right)}{f_0\ \Delta P^l} + \frac{2\sum_{g}^{G} Sys_{g,t}^{iner}\Delta f^{db}}{f_0\ \Delta P^l}\right] \quad (19)$$

The steady-state frequency Δf_t^s is calculated through (20), depending upon load damping $Damp$, system PFR is assessed.

$$\Delta f_t^s = \frac{\Delta P^l - pfr_t^{tot}}{Damp\ Load_t} \le \Delta \bar{f}^s \quad (20)$$

C. PHES Scheduling

This section gives the PHES constraints for day-ahead scheduling. (13) and (14) gives the power generated $P_{p,t}^{turb}$ and consumed $P_{p,t}^{pump}$ by PHES unit p during generating and turbine mode and cf_p^{pump} conversion factor for water flow to depending upon the flow $Q_{p,t}^{turb}$ and $Q_{p,t}^{pump}$ respectively. cf_p^{turb} power produced and water-flow to power consumed respectively.

$$P_{p,t}^{turb} = cf_p^{turb}.Q_{p,t}^{turb} \quad \forall p,t \quad (21)$$

$$P_{p,t}^{pump} = cf_p^{pump}.Q_{p,t}^{pump} \quad \forall p,t \quad (22)$$

The water at upper reservoir $vol_{p,t+1}^U$ and lower reservoir $vol_{p,t+1}^L$ is calculated based upon its volume and water flow at time t given in (15) and (16). The volume at upper and lower reservoir is constrained by reservoir maximum and minimum limits as in (17) and (18). The water flow from during generating and pumping mode is constrained by (19) and (20).

$$vol_{p,t+1}^U = vol_{p,t}^U + Q_{p,t}^{pump} - Q_{p,t}^{turb} \quad \forall p,t \quad (23)$$

$$vol_{p,t+1}^L = vol_{p,t}^L + Q_{p,t}^{turb} - Q_{p,t}^{pump} \quad \forall p,t \quad (24)$$

$$vol_p^{L,min} \le vol_{p,t}^L \le vol_p^{L,max} \quad \forall p,t \quad (25)$$

$$vol_p^{U,min} \le vol_{p,t}^U \le vol_p^{U,max} \quad \forall p,t \quad (26)$$

$$0 \le Q_{p,t}^{turb} \le M_t Q_p^{max} \quad \forall p,t \quad (27)$$

$$0 \le Q_{p,t}^{pump} \le (1 - M_t) Q_p^{max} \quad \forall p,t \quad (28)$$

PFR and SI contribution from PHES is based upon its operating state as given in (21) and (22), where P_p^{max} is PHES maximum generation capacity.

$$pfr_{p,t} = M_t P_p^{max} - P_{p,t}^{turb} + P_{p,t}^{cons} \quad (29)$$

$$Sys_{p,t}^{iner} = \frac{\sum p\ \bar{P}_P H_P\ M_t}{f_0} \quad \forall t \quad (30)$$

The system total PFR and SI is given in (31) & (32).

$$pfr_t^t = \sum_g pfr_{g,t} + \sum_p pfr_{p,t} \quad \forall t \quad (31)$$

$$Sys_t^{tot} = Sys_{g,t}^{iner} + Sys_{p,t}^{iner} \quad (32)$$

Power balance equation is given in (33), based upon line transfer capability P_{ij},power from wind plants P_t^{wind}, PV plants P_t^{pv}, and generation from conventional units $P_{g,t}$, $Load_{i,t}$ is served connected at bus i at time t.

$$\sum_g P_{g,t} + Load_t^{shed} + P_t^{wind} + P_t^{pv} - Load_{i,t} = \sum_{j \in \Omega_i} P_{ij,t} \quad (33)$$

III. CASE STUDY

The proposed work is demonstrated using New England test system [14]. PV and wind units are incorporated to analyze the impact of different RES integration on post-fault system frequency dynamics. Hourly data of wind speed and PV irradiance for a day is considered using New England coordinates [15]. The total installed capacity of SG units is 8840 MW with a peak demand of 5748 MW. The data for nominal frequency f_0 (=60 Hz), maximum value of rate of change of frequency $\overline{RoCoF}$ (=2 Hz/sec), governor dead band Δf^{db} (=36mHz), maximum steady state frequency deviation $\Delta \bar{f}^s$ (=0.2Hz), load damping $Damp$ (=1%), and under frequency load shedding bound as f^{ufls} (=59.1Hz) is opted. The system PFR requirement is assumed to be 50% of the system largest generator. The capacity of PHES is takes as 200MW and relevant data is assumed from [16], fixed operating cost is assumed as 18$/Kw-h yearly [17]. PV and wind curtailment cost as 0.7$/MWh and 1$/MWh respectively [18].

The study examined two cases broadly: (i) PFR constrained generation scheduling with a bound on RoCoF and steady-state frequency limits. (ii) PFR constrained scheduling with no bounds on RoCoF and steady-state frequency. Under these two broader sections, five different cases are analysed: (i) Base case (case i) – conventinal units without RE integration (ii) case ii- Base case with 20% RES integration (iii) Case iii- base case with 30% RES integration (iv) case iv- Base case with 40% RES integration and (v) case v- Base case with 50% RES integration. All the aforementioned cases (ii)-(v) are analysed with and without PHES. The analysis is maintainly focussed on system frequency paparameter like RoCoF, frequency nadir and steady state frequency and its impact on system operating cost. The PFR availability in day-ahead is assured to maintain system security under inevitable events. The largest generator outage is considered at time t_5.

Fig.1. gives the load, wind and PV generation profile for a day in hourly frame. Wind and PV power generation shown is at 10% integration. Wind avialiability is variable and almost constant from $t_5 - t_{13}$ and PV is at its peak at time t_{13} and zero in initial and last hours of the day.

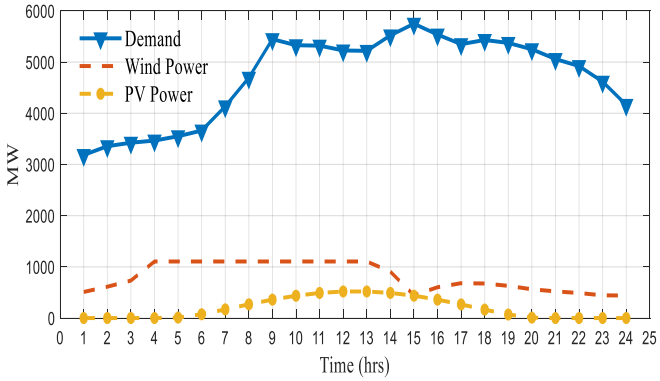

Fig.1. Load, wind and PV power profile for a day

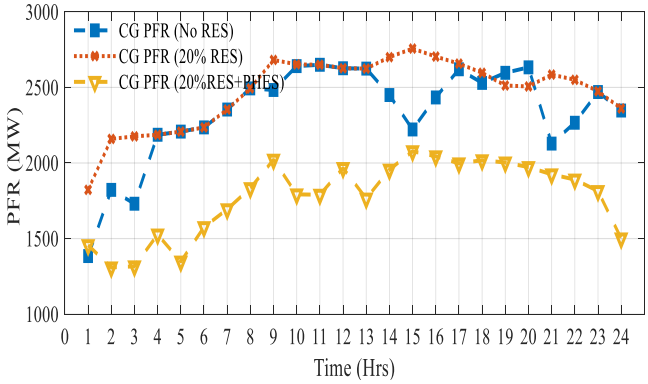

Fig.2. CG PFR share under 20% RES integration

System operating cost varies under different cases, as integration of RES in the system leads to SG displacement, and incorporation of PHES further declines the operating cost of system as PHES has negligible variable O&M cost. Thus, the overall system operating cost reduces.

TABLE I

OPERATING COST OF THE SYSTEM (in dollars)

Case	Without PHES	With PHES
Base case	2606027	-
Case -ii	2036930	2032334
Case- iii	1665624	1661104
Case- iv	1238284	1232338
Case- v	967201.2	963742.6

A. *Bounds on RoCoF and steady-state frequency limits*

In this section, along with basic SI and PFR constraints, bound on RoCoF as 2Hz/sec and change in steady-state frequency as 0.2 is taken. Simulation is carried on all the cases with and without PHES in the system. Results shows that at 20% and 30% RES integration (with and without PHES), system frequency is maintained during largest generator outage. However, with 40% and 50% RES integration (without PHES) system fails to maintain frequency limits. Although these limits can be attained on PHES integration. A single unit of PHES with 200 MW capacity is installed to analyses the system frequency characteristics.

TABLE II

SYSTEM PERFORMANCE

Case	Without PHES	Operating Cost ($)	With PHES	Operating Cost ($)
Base case	√	2606027	-	-
Case -ii	√	2037064	√	2032000
Case- iii	√	1665598	√	1661624
Case- iv	×	-	√	1232391
Case- v	×	-	√	961442

Table -II summarizes the system operating cost with strict bounds on frequency under different integration of RES.

The PFR contribution through conventional units significantly affected by RES integration. As seen in Fig.2. the PFR requirement in most of the instances is increased on RES integration, and same is reduced drastically on PHES integration. This shows that PHES integration lowers the burden on conventional units for PFR support. Thus, additional operating cost incurred due to additional commitment for PFRs reduces.

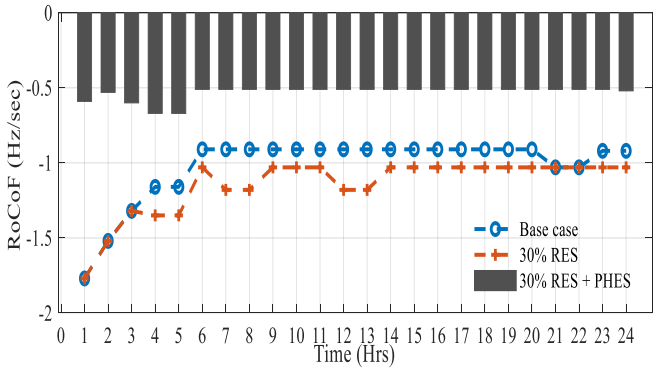

Fig.3. Rate of change of frequency for 30% RES integration

B. *Frequency response characterstics (no bounds on RoCoF and Steady-state frequency limits)*

The variation of SI under diffrerent integration is plotted in Fig.4, due to low availability of wind power and decreasing profile of PV power from t_{15}, CG are committed to balance of load in this period and hence SI is high comaparble with base case

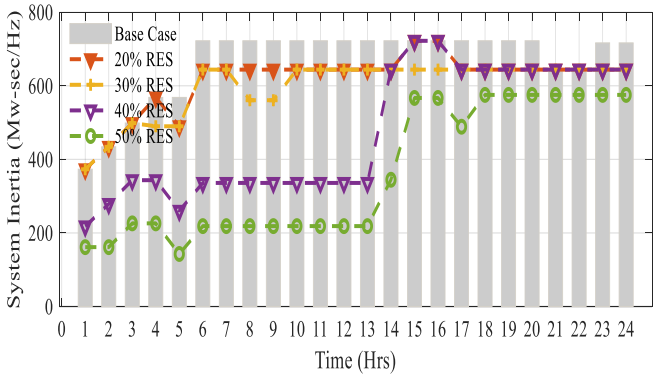

Fig.4. System inertia under different RES integration (with PHES)

The variation of SI at different dispatch impacts the system RoCoF. To maintain SI and thus RoCoF, PHES is incorporated in the system, impact of PHES on system RoCoF at 40% and 50% RES integration is shown in Fig.5 and Fig.6. It is depicted from the result that PHES improves the frequency deviation from -3 Hz/sec to -1.8 Hz/sec and in case of 50% integration from -5 Hz/sec to -2.31 Hz/sec.

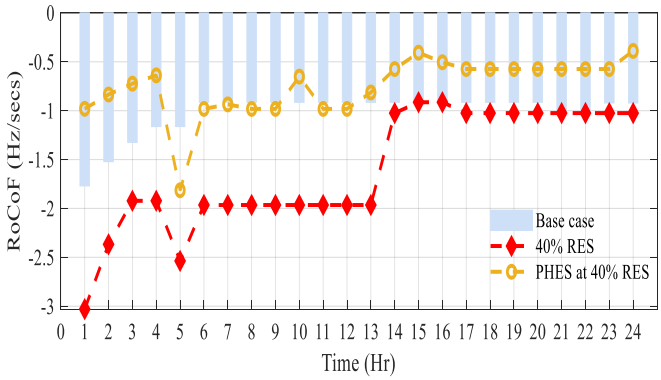

Fig.5. ROCOF at 40% RES integration with PHES

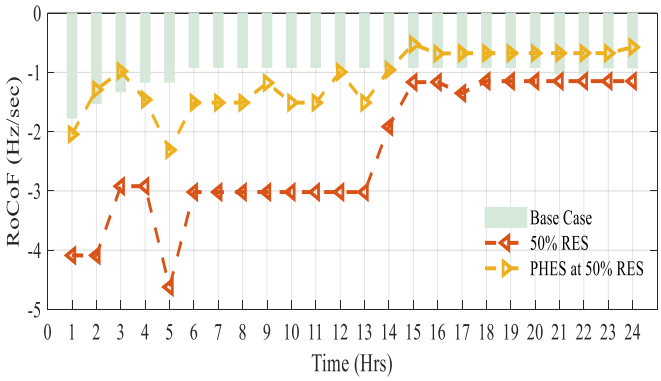

Fig.6. ROCOF at 50% RES integration with PHES

The steady-state frequency deviation under largest generator outage can be maintained by adequate PFR in the system. The system is scheduled in a way to provide sufficient response to stabilize the frequency to steady-state value. In present study PFR is adequately available to stabilize the frequency transients in all the under taken cases.

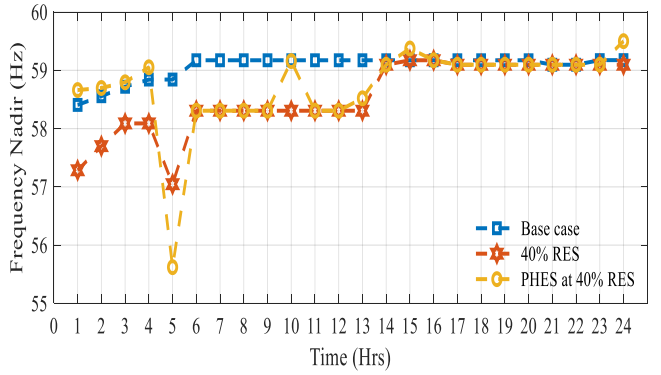

Fig.7. Frequency nadir at 40% RES integration with PHES

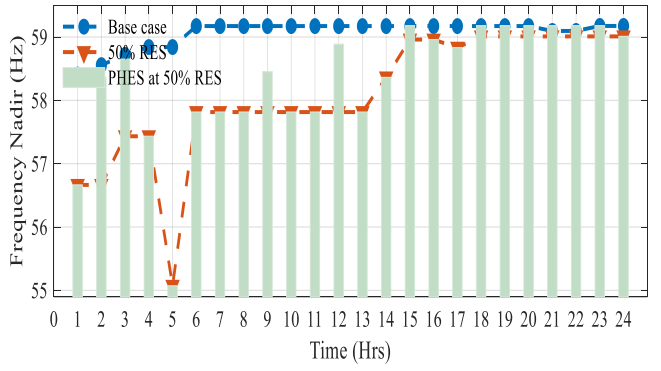

Fig.8. Frequency nadir at 50% RES integration with PHES

Similarly, Frequency nadir under different RES integration varies drastically, results in lower frequency nadir for increase in RES. The Fig. 7 and Fig. 8 shows the variation of frequency nadir at 40% and 50% RES integration. As can be depicted there is sudden fall in frequency nadir at time t_5 due to sudden outage at this time. Units fails to cope up the outage of largest generator and frequency nadir may cross UFLS limits.

Fig. 9. Shows the PFR and SI contribution by PHES. Depending upon the system frequency response requirement at different RES integration, PHES contributes. Case 1 shows is 20% RES integration, next at 30% integration and so on. There is no RES curtailment at 20% and 30%, however as integration percentage increases, RES is curtailed. There is no significant reduction of curtailment on PHES incorporation, due to system security constraints.

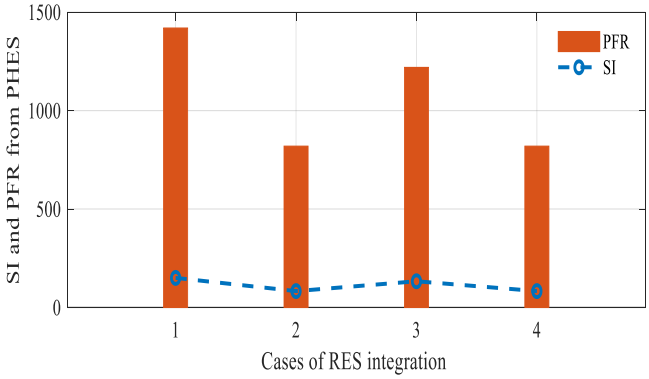

Fig.9. PFR and SI contribution from PHES under different RES integration

IV. CONCLUSION

This paper proposes SI and PFR constrained generation scheduling framework under different RES integration. The potential well established technology of bulk ESS, PHES is explored to address additional SI and PFR requirements. Five different cases with different RES integration are analyzed. The bounds on RoCoF and steady state frequency is used to examine the impacts of SI and PFR to stabilize the system under largest generator outage. It is observed that at lower percentage integration of RES in the system, CG units can provide the required response. However, at 40% and above penetration level even CG response fails to keep frequency in permissible range. Thus, in the present study, such cases of large RES integration, ESS like PHES plays a vital role in stabilising system frequency dynamics within range. System parameters like RoCoF, frequency nadir and steady-state frequency are analysed for their ability to control post-fault frequency dynamics and estimate the PFR requirement. Additional resources reduce the PFR contribution from CG and the additional schedules. Thus results in a reduction in overall system operating cost. As RES integration bears negligible O&M cost, results in the overall reduction of operating cost.

Proposed work has the potential to support SO in enhancing system PFR and SI adequacy under large-scale RE integration. This framework could be enhanced by incorporating other additional resources for low inertia power systems.

V. REFERENCE

[1]. Gannon, M., Swier, G., and Gordon, R.: "Emerging Rate-of-Change-of-Frequency problem in the NEM: Best-practice regulatory analysis of options," 2014, University of Melbourne, Melbourne

[2]. P. Kushwaha, V. Prakash, R. Bhakar, U. R. Yaragatti, A. Jain and Y. Sumanth, "Assessment of Energy Storage Potential for Primary Frequency Response Adequacy in Future Grids," 2018 8th IEEE India International Conference on Power Electronics (IICPE), JAIPUR, India, 2018, pp. 1-6.

[3]. Pengwei, D., and Matevosyan, J.: "Forecast system inertia condition and its impact to integrate more renewables," IEEE Trans. Smart Grid, 2018, **9**(2), pp. 1531–1533.

[4]. Wen, Y., Guo, C., and Kirschen, D. S. et.al: "Enhanced security-constrained OPF with distributed battery energy storage," IEEE Trans. Power Sys., 2014, **30**(1), pp. 98–108.

[5]. Hernánde, J., Bueno, P. G., and Sanchez-Sutil, F. C.: "Enhanced utility-scale photovoltaic units with frequency support functions and dynamic grid support for transmission systems," IET Renew. Power Gener., 2017, **11**(3), pp. 361–372.

[6]. Attya, A.B.T., and Hartkopf, T.: "Utilising stored wind energy by hydro-pumped storage to provide frequency support at high levels of wind energy penetration," IET Gener. Transm. Distrib., 2015, **9**(12), pp. 1485–1497.

[7]. Delille, G., Francois, B., and Malarange, G.: "Dynamic frequency control support by energy storage to reduce the impact of wind and solar generation on isolated power system's inertia," IEEE Trans. Sustain. Energy, **3**(4), pp. 931–939.

[8]. Egido, I., Sigrist, L., Lobato, E., and Rouco, L.: "Energy storage systems for frequency stability enhancement in small-isolated power systems," Energies, 2015, pp. 1–6.

[9]. Yang C, Jackson RB. Opportunities and barriers to pumped-hydro energy storage in the United States. Renew Sustain Energy Rev 2011;15(1):839–44.

[10]. Ela, Erik, et al. Role of pumped storage hydro resources in electricity markets and system operation. No. NREL/CP-5500-58655. National Renewable Energy Lab.(NREL), Golden, CO (United States), 2013.

[11]. Botterud, Audun, Todd Levin, and Vladimir Koritarov. Pumped storage hydropower: benefits for grid reliability and integration of variable renewable energy. No. ANL/DIS-14/10. Argonne National Lab.(ANL), Argonne, IL (United States), 2014.

[12]. F. Fernandes, J. A. M. Sousa, J. Santana and J. Lagarto, "Scheduling of a Pumped-Storage Hydro in the Day-Ahead Market and in the Secondary Reserve Market," *2018 15th International Conference on the European Energy Market (EEM)*, Lodz, 2018, pp. 1-5.

[13]. F. Teng, V. Trovato and G. Strbac, "Stochastic Scheduling With Inertia-Dependent Fast Frequency Response Requirements," in *IEEE Transactions on Power Systems*, vol. 31, no. 2, pp. 1557-1566, March 2016.

[14]. Krishnamurthy, D., Li, W., & Tesfatsion, L.: "An 8-zone test system based on ISO New England data: development and application," IEEE Trans. Power Syst., 2016, **31**(1), pp. 234–246

[15]. Wind speed and PV irradiance data, [Online]. Available: http://www.soda-pro.com/.

[16]. "Pinnapuram integrated renewable energy with storage project (IRESP) [Online].Available: http://environmentclearance.nic.in/writereaddata/Online/TOR/16_Apr_2018_13182853391O82IHRPinnapuramPFRFinalToR.pdf

[17]. Energy, U. S. "Updated Capital Cost Estimates for Utility Scale Electricity Generating Plants." *Information Administration*(2013).

[18]. Trovato, V., Bialecki, A., and Dallagi, A.: "Unit commitment with inertia-dependent and multi-speed allocation of frequency response services," IEEE Trans. Power Sys., 2018, **34**(2) pp. 1537-1548